

## Variscan Shearing in the Moldanubian of the Bohemian Massif: Deformation, Gravity, K-Ar and Rb-Sr Data for the Choustník Prevariscan Orthogneiss

By PETR RAJLICH, JEAN J. PEUCAT, JAN KANTOR & JOSEF RYCHTÁR\*)

With 16 Text-Figures and 8 Tables

*Bohemian Massif  
Orthogneisses  
Variscan shearing  
Rb-Sr dating  
Normal faulting  
Strain data  
Quartz c-axes fabric  
Gravimetry*

### Contents

Zusammenfassung .....	579
Abstract .....	580
1. Introduction .....	580
2. The Moldanubian of the Bohemian Massif and Geological Setting of the Choustník Orthogneiss .....	581
2.1. Geology and Petrology of the Choustník Orthogneiss and of the Host Rocks .....	581
2.2. Shearing of the Granite .....	584
2.3. Strain Analysis .....	585
2.4. Quartz c-axes Preferred Orientation .....	587
2.5. The Shape of the Orthogneiss Body from Gravity Interpretation .....	587
2.6. Rb-Sr Dating .....	589
2.7. K-Ar Cooling Ages of Muscovite and Biotite .....	590
3. Discussion .....	592
4. Conclusion .....	593
Acknowledgements .....	593
References .....	593

## Variszische Schertektonik im Moldanubikum der Böhmisches Masse: Deformations-, Schwere-, K-Ar- und Rb-Sr-Daten des variszischen Choustník Orthogneises

### Zusammenfassung

Die Struktur der 90 m mächtigen Klippe von prävariszischem Choustník Granit ist während einer nach S bis SSW gerichteten variszischen Überschiebung, gefolgt von Abschiebungen nach NW, entstanden. Die Überlagerung der beiden Schersysteme spiegelt sich in der Entwicklung der manchmal stark linearen Gefüge in den Tektoniten der ersten Phase und in der amphibolit-faziellen Mylonitisierung in der späteren Phase wider. Ein steiler Scherungsgradient und diskrete Scherzonenentwicklung ist für die späteren Scherzonen typisch.

Der höchste  $\Gamma$ -Wert ist 3,6, die Strainellipsoide variieren von constrictional bis oblate. Die jüngsten (K/Ar-) Kühlungsalter zeigen 280 Mio Jahre. Die Orthogneise mit einer ähnlichen Textur können als Indikatoren für variszische kinematische Geschichte benutzt werden. Der Choustník-Orthogneiss ist ein Beispiel der variszischen, polyphasen Kinematik im moldanubischen Terrane.

\*) Authors' addresses: Dr. PETR RAJLICH, Institute of Geology, Czechoslovak Academy of Sciences, Rozvojová 135, 165 00 Prague 6-Lysolaje; JEAN J. PEUCAT, Centre Armoricaïn des Études du Socle, Campus Beaulieu, Avenue Général Leclerc, 350 42 Rennes, France; JAN KANTOR, Geologický ústav Dionýza Štúra, Mlynská dolina 1, Bratislava, Czechoslovakia; JOSEF RYCHTÁR, Geofyzika n.p., Poděbradova 102, 602 00 Brno, Czechoslovakia.

## Abstract

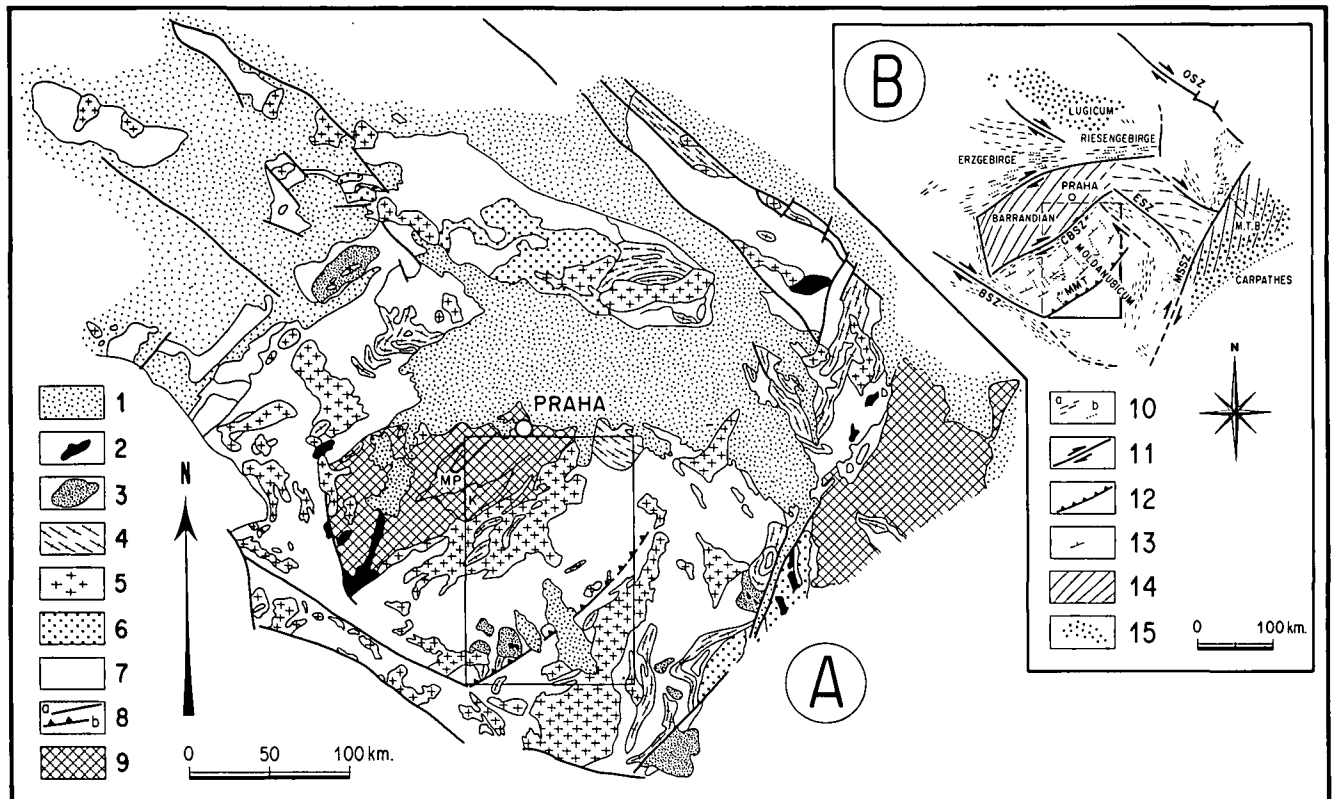
The structure of the 90 m thick thrust klippe of the Prevariscan porphyry Choustník granite in the Moldanubian of the Bohemian Massif originated during Variscan shearing events with an early S to SSW oriented, thrusting and later normal top to the NW faulting. Superposition of both types of shearing is reflected in the development of the often strongly linear mylonitic fabric during the earlier, and by the mylonitization in the amphibolite facies metamorphism in the later shearing stage. A steep shear strain gradient and discrete shear zone development are characteristic for the younger event. Deformation produced quartz c axes orientations with relict asymmetrical crossed and oblique girdle fabrics. Shear strains up to  $\Gamma = 3.6$  are found in the older tectonites and the strain ellipsoids range from constrictional to oblate types. The (K/Ar) cooling ages range up to 280 Ma. Orthogneisses with similar textures in the Bohemian Massif can be used as markers of the Variscan kinematic history. The Choustník orthogneiss provides an example of the Variscan polyphase kinematics in the Moldanubian terrane.

## 1. Introduction

The principal structural and kinematic units of the Bohemian Massif have been characterized using stretching lineations, foliations and bulk kinematics, combined with other geological data (RAJLICH, 1987; RAJLICH & SYNEK, 1987; FRANKE, 1989; MATTE et al., 1990 etc.). The most striking conclusion following from this study is the importance of ductile strike-slip zones that divide the massif into a mosaic of smaller blocks with contrasting sedimentary sequences and differing structural assemblages (Fig. 1, Table 1). The inner segments separated by the NE-SW strike-slip zones underwent both transpression and crustal thickening through thrust stacking, and transtension and normal faulting. Differing deformation and mobility can also be observed in these segments as first noted by STILLE

(1949). Except for the Barrandian which is composed mostly of weakly metamorphosed Upper Proterozoic rocks, fine-grained granulites and eclogites are present in all the above-mentioned units.

The Variscan granites are the important unifying element of the Late Palaeozoic development. The oldest are the durbachites-melanocratic biotite and amphibole granites and syenodiorites which give 336 Ma. cooling ages using  $^{39}\text{Ar}/^{40}\text{Ar}$  (MATTE et al., 1990). These are followed by 330 Ma. granodiorites. The cooling ages for the whole Massif based on K-Ar dating (ŠMEJKAL & MELKOVÁ, 1969) range from 390 to 260 Ma. They are partly contemporaneous to shearing. No zonal pattern for the chemistry in the whole area has been discerned (KLOMINSKÝ & DUDEK, 1978). The tectonics does not, at present, permit a clear definition of a single suture zone in this area, as suggested by the work of



Text-Fig. 1.

Geological scheme of the Bohemian Massif (A) with principal kinematic units (B).

1 = The undeformed cover (Upper Carboniferous and later rocks); 2 = Mafic and ultramafic intrusive complexes; 3 = Granulites; 4 = Orthogneisses; 5 = Undeformed Variscan granites; 6 = Cadomian (600–550 Ma.), mostly undeformed granites; 7 = Metamorphosed units ( $\approx 2000$  Ma.); 8a = Faults, b = Thrusts; 9 = Upper Proterozoic, mostly weakly metamorphosed rocks; 10a = Stretching lineations related to older shearing event, b = Normal fault stretching lineations; 11 = Principal ductile strike-slip zones; 12 = Principal thrusts; 13 = Strike and dip of normal faults in extended areas; 14 = Strike of fold axes in transpressed regions; 15 = Zones of the Cadomian calc-alkaline granites and older migmatites.

Table 1.

Phanerozoic rocks in the principal tectonic units of the Bohemian Massif.

E = eclogites, G = granulites, GS = garnet serpentinites, GA = Garnet amphibolites, O = orthogneisses, P = Paragneisses, MG = migmatites, MS = micaschists, MA = marbles.

	Moldanubicum	Bohemicum	Moravicum	Thuringicum – Lugicum
Proterozoic	Lower Upper	Siltstones, shales, conglomerates, bimodal volcanics		
Cambrian		Conglomerates, shales, Acid volcanics		Conglomerates, marbles
Ordovician		Quartzites, shales, mafic volcanics		Quartzites, shales
Silurian		Shales, limestones, mafic volcanics	Shales, limestones	
Devonian	Marbles?	Limestones, shales	Conglomerates, shales, quartzites, bimodal volcanics, marbles and limestones	Marbles, bimodal volcanics, shales
Carboniferous	Lower		Conglomerates, graywackes, shales	Conglomerates, shales
	Upper	Arcoses, coal seams	Arcoses, coal seams	Conglomerates, acid volcanics
Metamorphics	E, G, GS, GA, O P, MG, MS, MA	MS, A	G, E, MS, GA, P, MG, MA, GA, O	E, G, GS, O, P, MG, MS, MA, GA

BARD et al. (1980), BEHR (1978, 1980), MATTE (1983) and others. It is probable that a significant amount of pre-Variscan crust and relatively minor amounts of oceanic crust were involved in the Hercynian structures, as suggested by BADHAM (1982) and CHALOUPEK (1986). Chronological correlation of kinematical phases over various units-terrains is needed. From this point of view, the position of the Bohemian Massif in the European Variscides is crucial and demonstrates that the development of European Variscides is not yet fully understood. Nevertheless, the geological evidence, (KREBS, 1977; ZOUBEK et al., 1988) and existing geochronological data (VAN BREEMEN et al. 1982) yield features comparable to other parts of Hercynian Europe, e.g. 2 B.Y. old paragneisses, calc-alkaline and alkaline magmatism of Cadomian age and Variscan shearing events followed by formation of large granitic batholiths.

The aim of this paper is to demonstrate that the determination of the Variscan kinematic history in the various segments of the Bohemian Massif can be carried out using markers (MARQUER, 1990) such as coarse-grained, alkali-feldspar granites that are mostly transformed into orthogneisses and which are present in several parts of the Bohemian Massif: eg. Erzgebirge, Moldanubian (SVOBODA et al., 1966), Moravian zone (ŽELAZNIEWICZ, 1988), Rumburk granite (OBERC-DZIEDZIC, 1988) and others. A typical example with the best-preserved original features is the Choustník orthogneiss that characterizes the tectonics of the Moldanubian region.

## 2. The Moldanubian of the Bohemian Massif and Geological Setting of the Choustník Orthogneiss

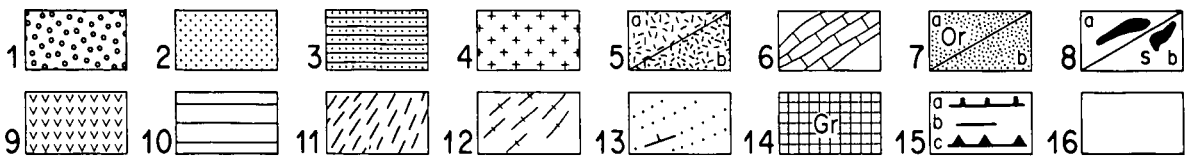
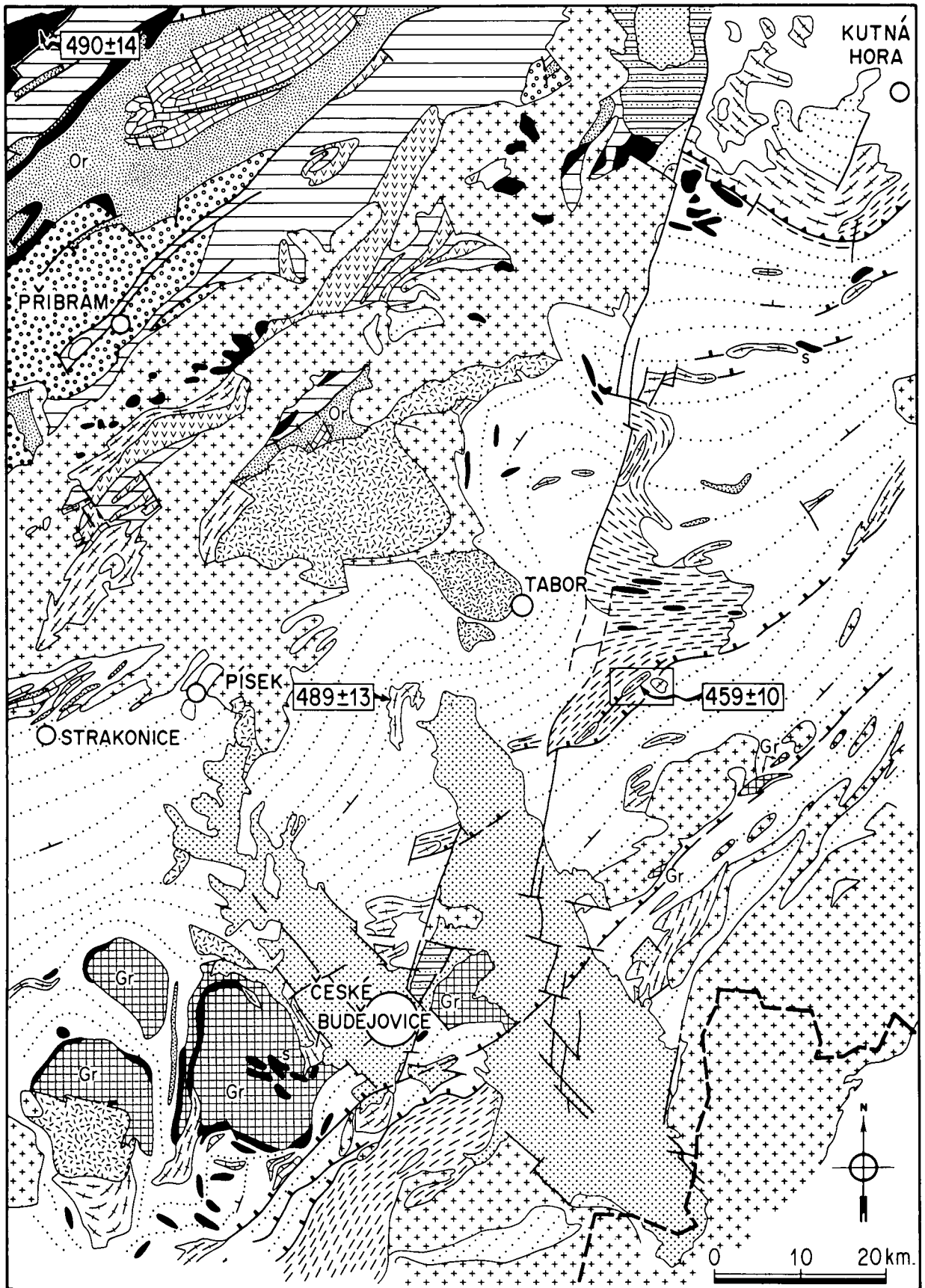
High grade regional metamorphism at garnet amphibolite conditions, the frequent occurrence of granitic intrusions, cordierite migmatites and the sillimanite rich paragneisses as well as the lack of unmetamorphosed older Palaeozoic sedimentary cover, are typical

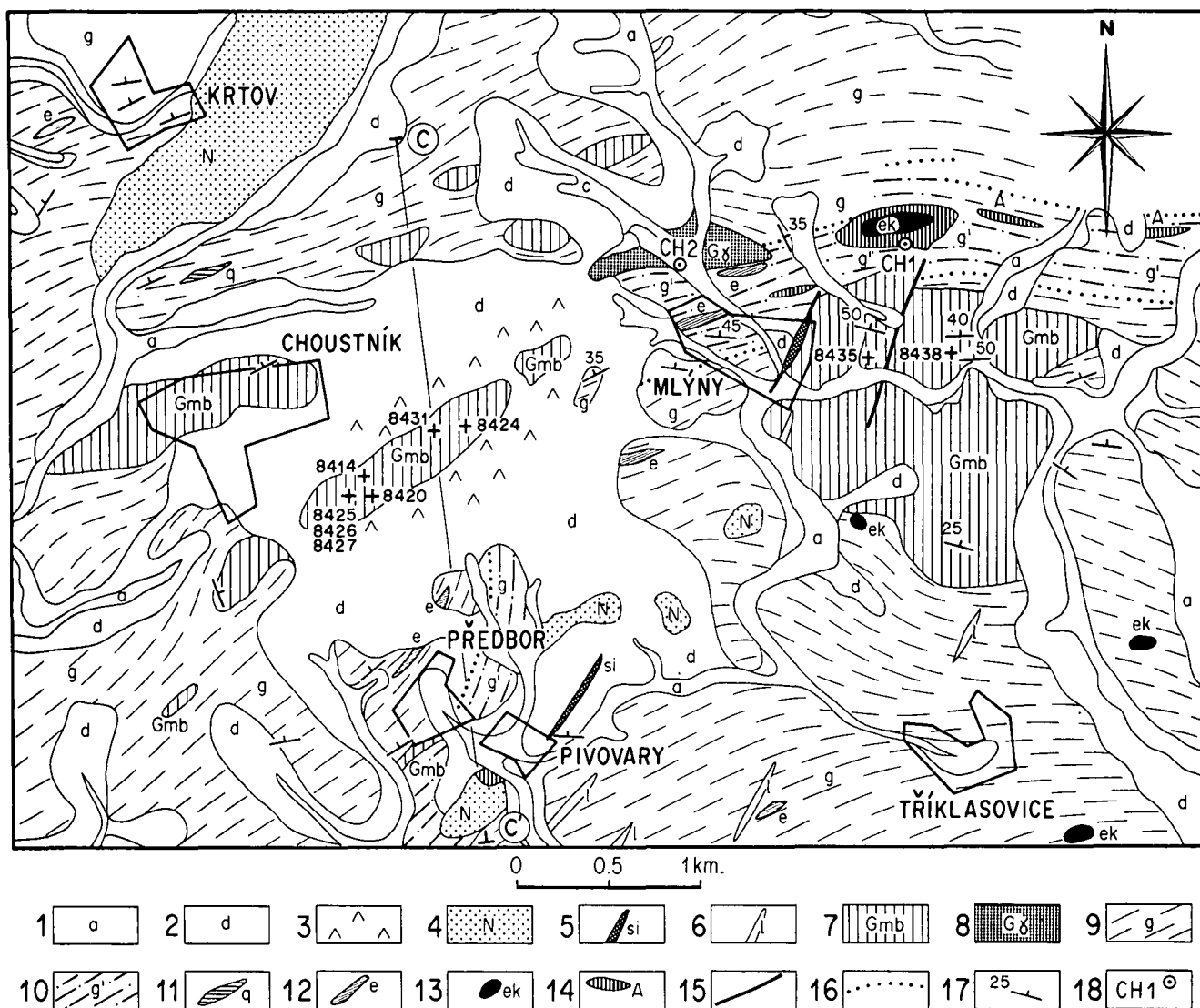
of the whole Moldanubian area (ZOUBEK et al., 1988). The area is divided by the Central Moldanubian pluton into two parts; the eastern part contains mostly N-S trending lineations and is not affected by NW-SE lineations that are related to normal ductile faulting and which are characteristic of the western part, occurring just prior to and partly contemporaneously with the granite intrusions.

Two principal groups of paragneisses, the Varied and Monotonous groups with and without "varied" inclusions such as marbles, amphibolites, graphitic quartzites etc., can be distinguished in the western part. In addition to paragneisses, extensive areas of micaschists occur here (Fig. 2), but they do not occupy a unique structural geometrical position. They are found in an inverted metamorphic position beneath the granulites in the southern Moldanubicum which have been thrust in the earlier Variscan from N to S, similar to the major suture in the French Massif Central where thrusting of the amphibolite-leptynite rocks over micaschists has been described in the Marvejols area (MATTE & BURG, 1981). Another micaschist area is found in the region of E-W ductile faults fanning to the West in the Centre of the Moldanubian (Fig. 2). This micaschist unit formed of muscovite-biotite and two mica paragneisses contains numerous "varied" inclusions such as marble, calc-silicate rocks, amphibolite ± garnet, granite, eclogite, and orthogneiss (STUR, 1858; ANDRIAN, 1863; KLEČKA et al., 1986). It is here that the Choustník orthogneiss crops out.

### 2.1. Geology and Petrology of the Choustník Orthogneiss and of the Host Rocks

A number of muscovite-biotite orthogneiss bodies, several kilometres in size, within the foliation of the surrounding paragneisses and mica-schists are found in the vicinity of the villages of Choustník and Mlýny (Fig. 3). The general direction of the long axis of these bodies is NE-SW to E-W, following the general strike, orientation of the outcrop of micaschists which show northerly dips up to 45°. The whole belt is accom-





Text-Fig. 3.

Geological map of the Choustník orthogneiss, after ZIKMUND (1983), modified.

1 = Alluvial plains; 2 = Deluvial aprons; 3 = Rock taluses; 4 = Neogene sediments; 5 = Quartz lodes; 6 = Aplites, leucogranites; 7 = Orthogneisses; 8 = Isotropic alkali - feldspar granites; 9 = Muscovite-biotite paragneisses - micaschists; 10 = Muscovite-biotite micaschists with varied inclusions; 11 = Biotitic quartzites; 12 = Marbles and erlans; 13 = Eclogites; 14 = Amphibolites; 15 = Faults verified and presumed; 16 = Petrographical boundaries; 17 = Strike and dip of foliations; 18 = Structural borehole.

panied by ultramafic and mafic rocks such as eclogites, serpentinites and garnetiferous amphibolites, which also define one of the important tectonic contacts between the micaschists on the NW and paragneisses to the SE within the Moldanubian. In spite of their textural and structural diversity (KREJČI, 1877; ŠAFRÁNEK, 1878; BERNARD, 1909; ČECH et al., 1962), the orthogneisses show a rather homogeneous mineralogical composition and can be classified (considering their position in the AQP diagram, IUGS subcommission 1973) as alkali-feldspar granites, with some points falling in the syenogranite field. In their mafic mineral contents, they lie on the boundary between leucocratic and normal granites. The textural diversity of the rocks

is a result of the degree and age of shearing and of the degree of later recrystallization. The groups of relict granites and porphyries can be distinguished in principle from the group of orthogneisses. The porphyric muscovite-biotite granites contain quartz, microcline, albite, biotite and muscovite with accessories such as plagioclase, tourmaline, apatite, zircon and ore minerals. The automorphic K feldspar/orthoclase phenocrysts with 1.5x3 cm grain size are composed mostly of a fine-grained mixture of albite and microcline with relicts of K-feldspars (ZIKMUND, 1983). Recrystallized nuclei of perthites are occasionally preserved. The feldspars in the matrix were affected in the same manner. Quartz forms the xenomorphs, with clear smoky grains,

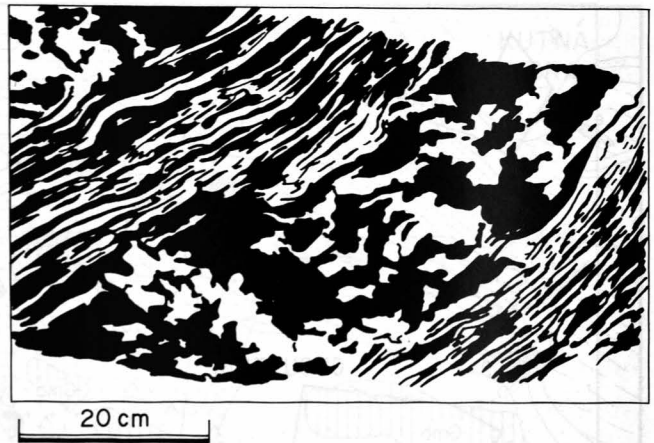
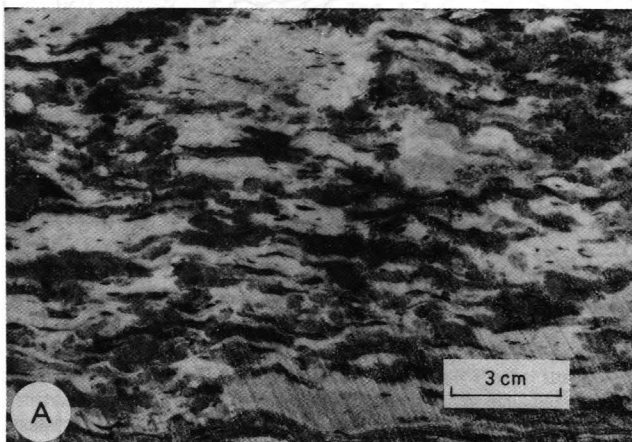
Text-Fig. 2. Schematic geological map of the western part of the Moldanubian.

1 = Lower Cambrian conglomerates; 2 = Cretaceous basins; 3 = Permian sandstones; 4 = Hercynian granites; 5 = Melanocratic biotite and amphibole granites and syenodiorites; 6 = Limestones; 7 = Quartzites in metamorphic units, Or = Ordovician quartzites in Barrandian and roof pendant of Central Bohemian pluton; 8 = Mafic rocks and volcanites, a = Unmetamorphosed volcanites in older Paleozoic, S = Eclogites and garnet peridotites, b = Amphibolites; 9 = Upper Proterozoic felsic and bimodal volcanites; 10 = Unmetamorphosed or weakly metamorphosed Upper proterozoic sediments; 11 = Micaschists; 12 = Orthogneisses; 13 = Paragneisses and migmatites with strike and dip of foliations; 14 = Granulites; 15: a = Thrust and normal faults, b = Faults, c = Low angle normal faults; 16 = Area studied.

2 to 8 mm in size. These primary magmatic grains are mostly recrystallized and represent small, tooth-shaped, undulating aggregates. The reddish-brown biotite forms 2 to 5 mm-large accumulations of variably oriented flakes that are sometimes intergrown with muscovite. It contains zircon and apatite and transformation into muscovite and chlorite is often visible. The An 26–28 oligoclase constitutes up to 1 to 3 % of the rock. The very coarse-grained porphyries represent a less widespread variety of rocks. Their boundary with the relict granite is magmatic-diffuse accentuated by biotite schlieren and by the accumulation of large K-feldspar phenocrysts at the endocontact. The size of phenocrysts may exceptionally attain 2×5×8 cm and, together with the K-feldspars of the matrix, they were transformed into an albite-microcline mixture, in a manner similar to that of the granites. But, because of the larger crystal size, this transformation is mostly limited to the outer margin. In addition to the above-mentioned rock types, there are dykes forming pegmatites and aplites of fine-grained, muscovite-biotite granite with tourmaline, with a mean thickness of 30 cm.

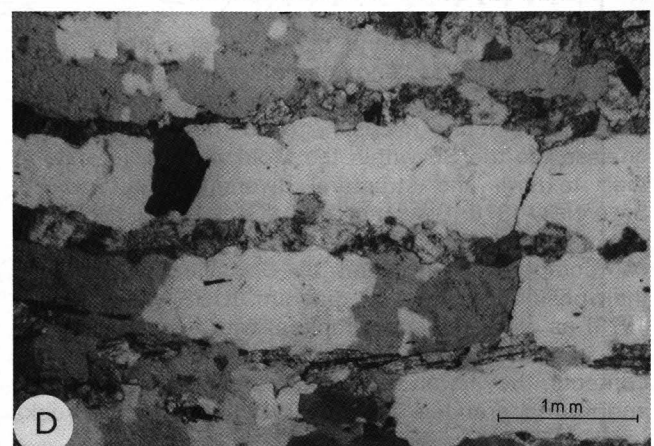
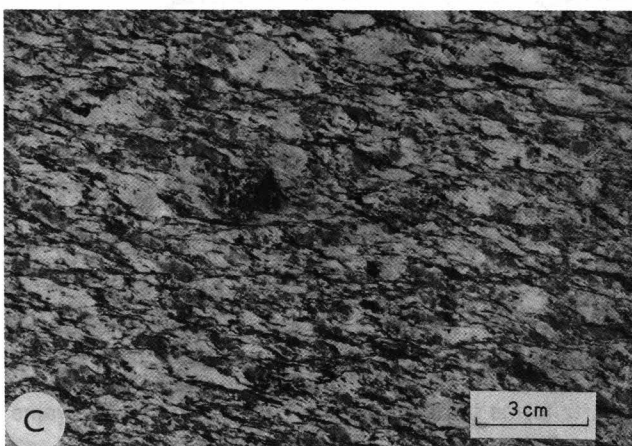
## 2.2. Shearing of the Granite

The type of orthogneiss developed depends on the ductility of the shearing process, and two principal events can be discerned:



Text-Fig. 4.  
Example of the ductile shearing of the Choustnik orthogneiss.  
Texture corresponds to deformation field above 550°C (GAPAI, 1989).

a) An earlier ductile thrusting, which transformed the granites and porphyries in places into strongly linear tectonites (Fig. 5A) indicating at least the amphibolite facies metamorphism during deformation (GAPAI, 1989a,b). During subsequent metamorphism these rocks could be recrystallized, with the formation of muscovite at the expense of biotite, and further albitization.

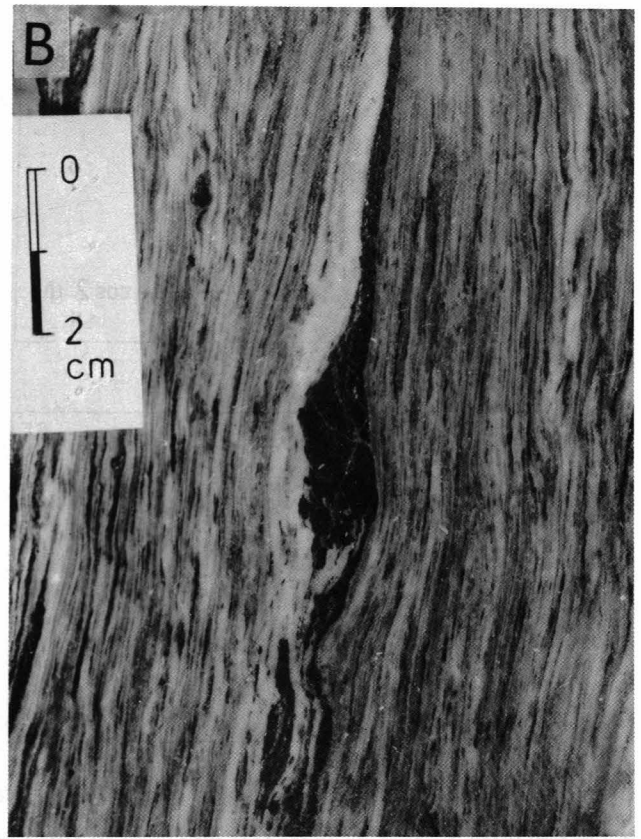
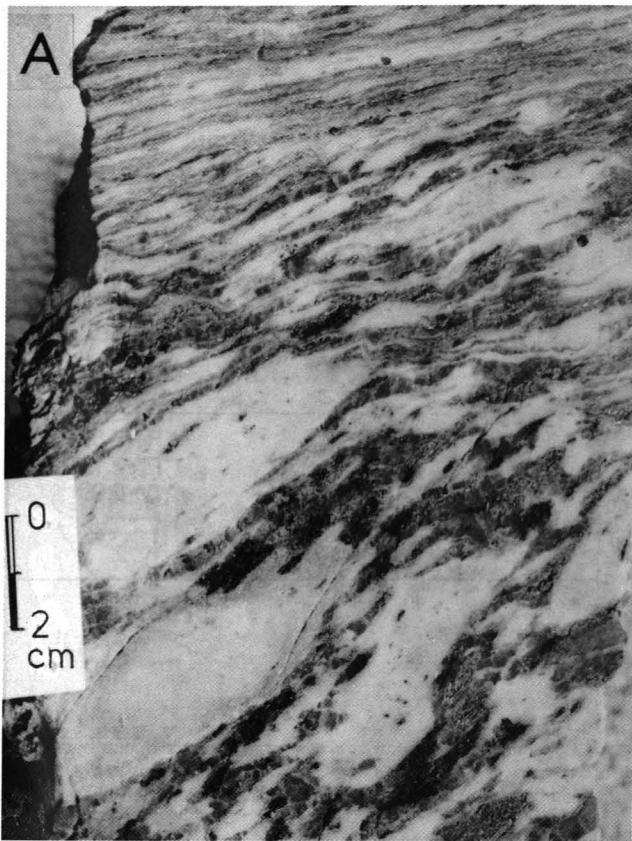


Text-Fig. 5.

Macro- and microscopic views of Choustnik orthogneiss.

- A) Texture of the ductile deformed Choustnik granite in the first stage of the shearing, note the less deformed quartz grains.
- B) Isotropic parts of the orthogneiss affected by normal fault shear zone with mylonitic structure in the central part.
- C) S & C mylonite structures in the granite oblique to the stretching structure Text-Fig. 5A.
- D) Quartz ribbons enveloped in the fine grained mylonitized fabric of feldspars and biotite; c-axes preferred orientation diagram of this sample is in Text-Fig. 14-403.





Text-Fig. 6.

Textural patterns of Choustník orthogneiss.

- A) Shear zone section with the ribbon quartz and albitized rims of large phenocrysts.  
 B) Central part of the shear zone with the concentrated tourmaline.

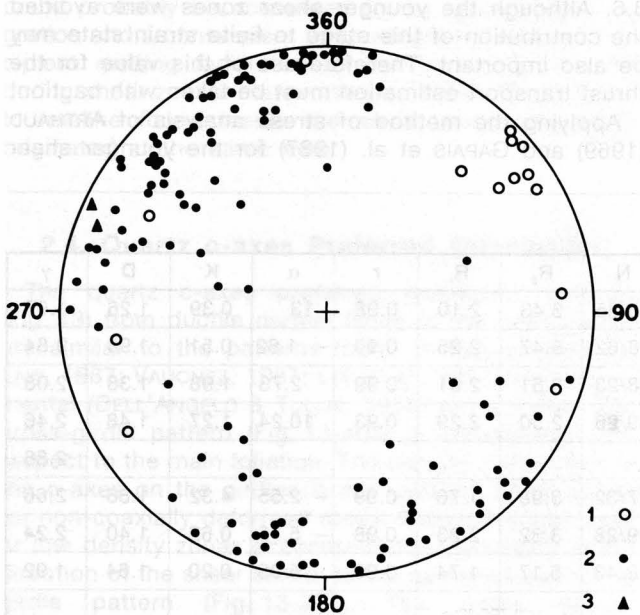
b) A later brittle-ductile normal faulting. The fabric varies from strongly ductile stretched minerals (Fig. 4) to mylonites (Fig. 5B) and S&C granites (Fig. 5C).

Many examples of superposition of both these types of shearing can be found in the field (Fig. 5). The mineralogical composition of the rocks in the younger

shear zones (not affected by the muscovitization) is the same as that of the relict granites. The brown biotite is often recrystallized and contains frequent spindles of exsolved rutiles (sagenite). Tourmaline is mostly automorphic, often with poikilitic texture. Bands of fine-grained panxenomorphic mixtures of albite, microcline and plagioclase (An 26–30) envelop the quartz ribbons (Fig. 5D) forming an L-S tectonite. The biotite has different pleochroic colours (green-brown) from those in the surrounding relict metagranites. It is associated with newly-formed muscovite in fine-grained streaks. The annealing structures can be observed in the formerly mylonitic fabric (Fig. 5C).

The foliation of the surrounding paragneisses and micaschists developed mainly in the first shearing stage, as can be seen from the conformity of the lenses of orthogneisses with the metamorphic schistosity in the whole area.

The stretching lineation inside the orthogneiss is reflected in the preferred orientation of feldspars and micas which define also the tectonic foliation (PATERSON et al., 1989). The lineation is oriented N–S to NW–SE (Fig. 7). In the surrounding quartzites and paragneisses N of the orthogneiss, the stretching lineation is oriented NE–SW and subhorizontal.



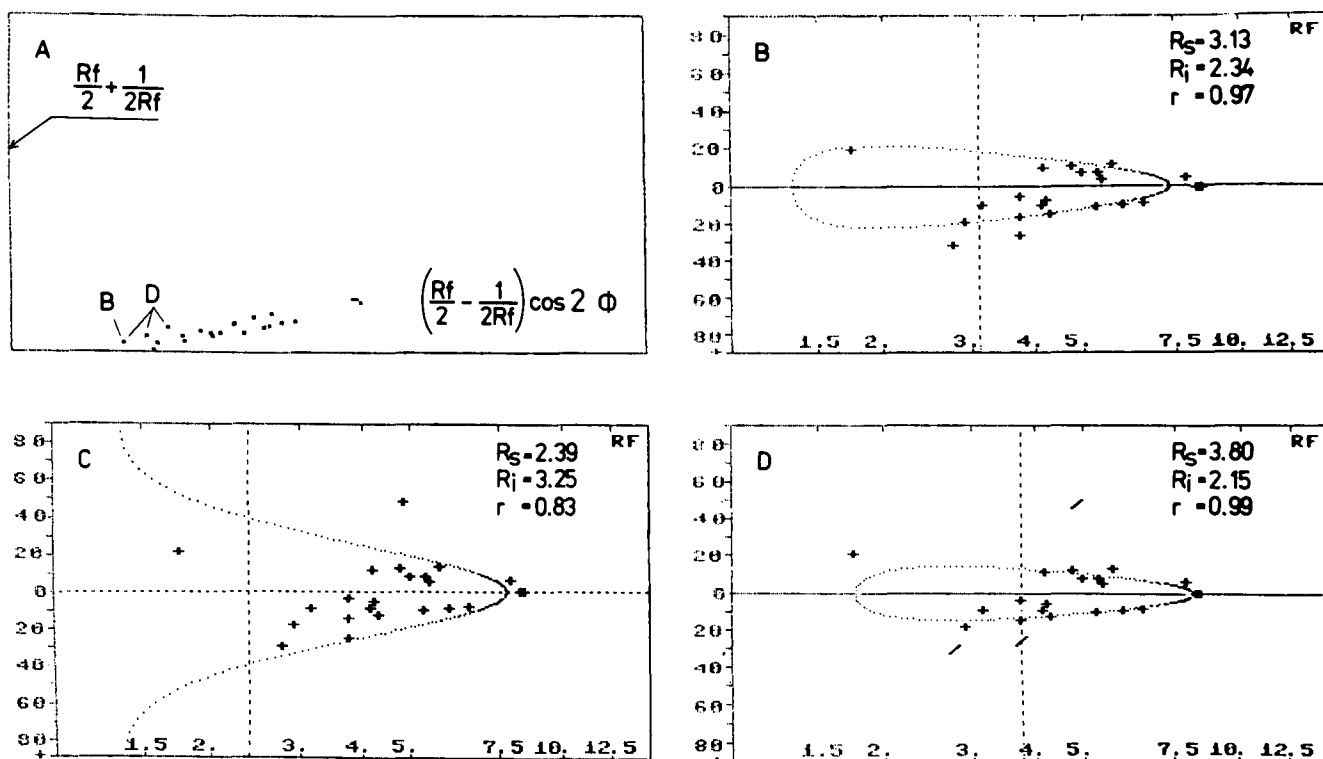
Text-Fig. 7.

Stretching lineations and fold axes of the area.

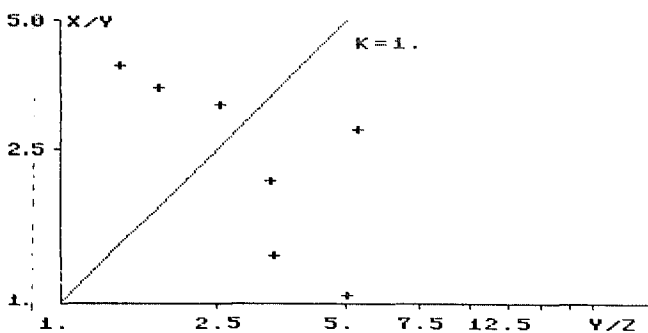
- 1 = NE–SW lineations and fold axes; 2 = NW–SE lineations; 3 = younger stretching lineations.

### 2.3. Strain Analysis

Strain analysis was carried out on deformed feldspar phenocrysts, quartz grains and tourmaline nodules, using the method of YU & ZHENG (1984) as modified by



Text-Fig. 8. Example of the use of linearization formula and line fitting for the  $R_f/\phi$  data with onion curves resulting from the successively discarded anomalous  $R_i$  values (B, D). C = all data; B and D = onion curves and finite strain values for sample with excluded anomalous data (oblique bars).



Text-Fig. 9. K-graph of the measured strain ellipsoids.

RAJLICH (1989) (see Table 2, Fig. 8). The linear data array corresponding to identical initial ellipticity was chosen from the measured set and the regression line was fitted. The tightness of the fit is controlled by the correlation coefficient (Table 2). The strain ellipsoids plot into the constrictional, plane strain and flattening fields (Fig. 9). The initial ellipticity ( $R_i$  = mean long and short axis ratio) of feldspar phenocrysts is around 2. The largest strain found corresponds to a  $\Gamma$ -value of 3.6. Although the younger shear zones were avoided the contribution of this stage to finite strain state may be also important. Therefore use of this value for the thrust transport estimation must be taken with caution.

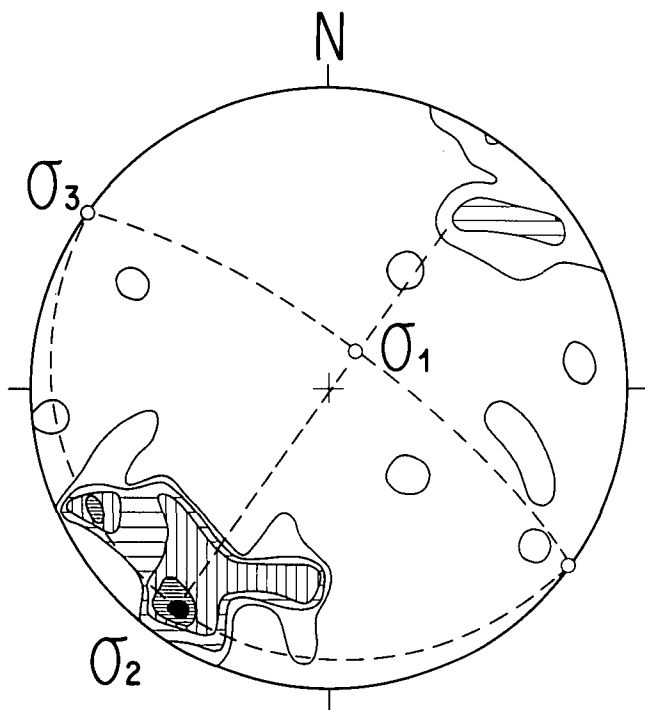
Applying the method of stress analysis of ARTHAUD (1969) and GAPAIS et al. (1987) for the younger shear

Table 2. Strain data for the Choustnik orthogneiss.

		N	$R_s$	$R_i$	r	$\alpha$		N	$R_s$	$R_i$	r	$\alpha$	K	D	$\gamma$
1	XZ	17/17	4.57	1.78	0.99	- 0.16	YZ	43/35	3.43	2.10	0.98	13	0.39	1.26	1.67
2	XY	30/16	2.78	1.96	0.98	17.95	YZ	78/62	5.47	2.25	0.99	- 1.62	0.51	1.98	3.64
3	XZ	70/45	6.20	2.27	0.98	8.90	XY	28/23	3.51	2.01	0.99	2.73	1.98	1.38	2.08
4	XZ	69/66	7.95	2.12	0.99	- 0.79	YZ	39/26	2.50	2.29	0.93	10.24	1.27	1.48	2.46
5	XZ	55/45	10.04	2.16	0.99	7.07									2.86
6	XZ	79/70	8.96	1.99	0.99	1.27	XY	37/32	3.98	1.76	0.99	- 2.55	4.32	1.86	2.66
7	XZ	52/41	6.87	2.00	0.99	1.95	YZ	49/28	3.32	2.23	0.98	- 5.75	0.62	1.40	2.24
8*)	XZ	28/20	5.50	2.04	0.99	8.20	YZ	48/43	5.17	1.74	0.99	5.05	0.20	1.64	1.92
4**)	YZ	19/16	3.34	1.90	0.98	15.42									
9**)	XZ	18/15	3.81	2.12	0.98	17.19									1.44

\*) Tourmaline nodules.  
\*\*) quartz.





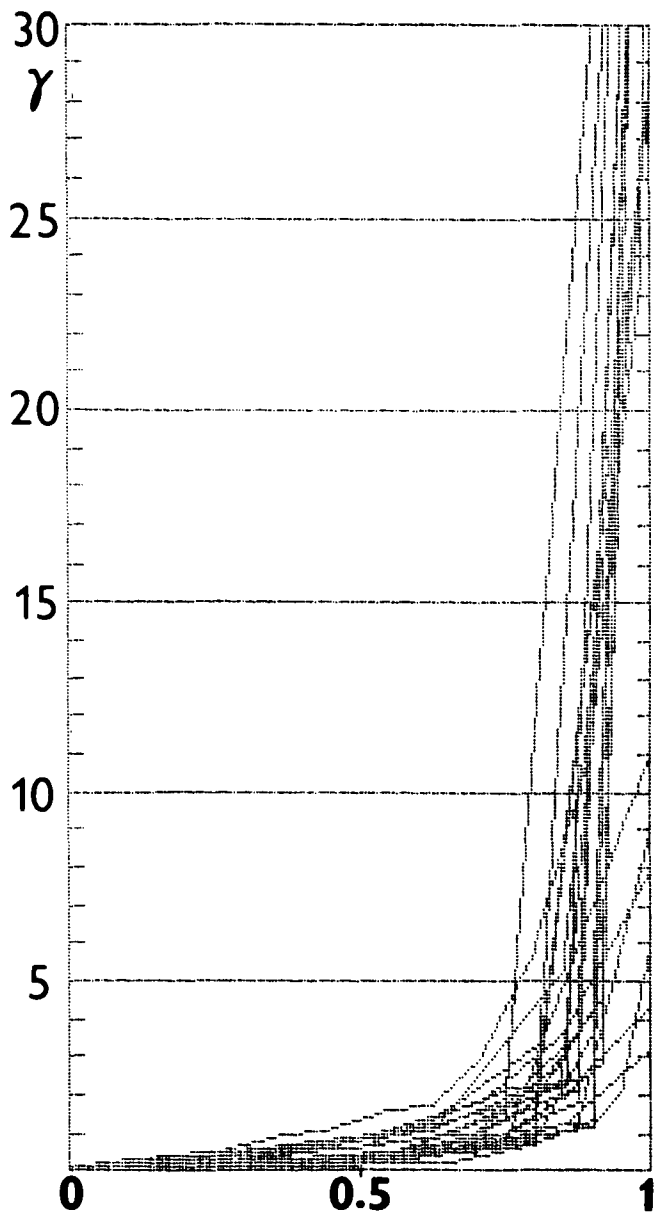
Text-Fig. 10.  
Stress axes orientation for the normal faulting shearing in the diagram of poles (B axes) to M-planes of ARTHAUD (1969).  
2 through 10 % density isolines of 46 points.

zones, the concentration of M-planes in the NW-SE direction indicates  $\sigma_1$  vertical and  $\sigma_2$  subhorizontal as well as plane strain symmetry for the shear zones spatial distribution (Fig. 10). This later stage can be interpreted as bulk simple shear normal faulting.

A characteristic feature of the younger shear zones is also a steep shear strain gradient (Figs. 11,12), indicating a rapid increase in ductility (softening) in the narrow movement zone, comparable to the necking of metals (DIETER, 1976). Temperatures above 550°C can be supposed for this deformation (GAPAIS, 1989). This could probably be accounted for by upward fluid migration and a consequent temperature increase with incipient melting facilitated by the fracturing of rocks during shear zone initiation (WHITE, 1984). The poikilitic tourmaline found inside the shear zones (Fig. 6A,B) originated at the same time.

#### 2.4. Quartz c-axes Preferred Orientation

The quartz c-axes preferred orientation patterns (Fig. 13) from ductile normal faults in the orthogneiss, are similar to the patterns found in natural (KNIPE & LAW, 1987; VAUCHEZ, 1987; LEE et al., 1987) and experimental (DELL'ANGELO & TULLIS, 1989) shear zones. The cross-girdle pattern (Fig. 13-403) is symmetrical with respect to the main foliation. The density distribution of the c-axes on the girdles is not uniform, as is typical for non-coaxially deformed rocks. Distinctive high and/or low density zones accentuate the asymmetry in the direction of the shear similar to the asymmetrical single girdle pattern (Fig. 13-221). The single density maximum pattern (Fig. 13-417) is similar to the fragmented single girdle pattern found by LEE et al. (1987) in sheared quartzites of the Northern Snake Range, Nevada and, compared to the experiments of



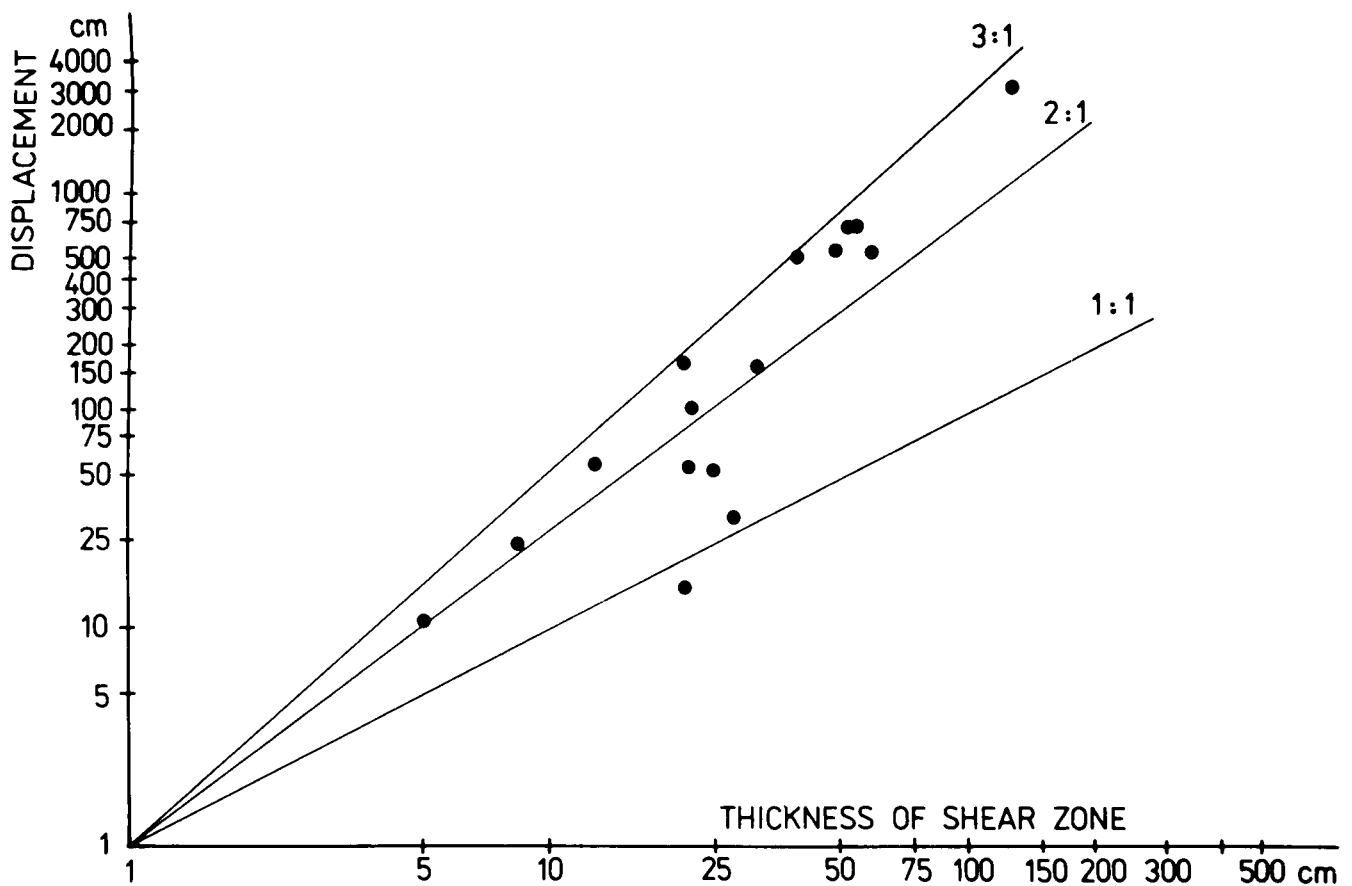
Text-Fig. 11.  
A  $\Gamma$ -curves of the measured shear zones with their width normalized to 1.

DELL'ANGELO & TULLIS (1989), it is typical for a transpressional deformation in which shear strain ( $\Gamma$ ) = 2.9 and pure shear compression ( $\epsilon$ ) = 60 %.

The c-axes orientation diagrams from the quartzites from the zone of ductile strike-slip show mostly strong obliquity and left hand shear sense and the compound-multistage fabric. The pattern found with exception of the diagram Fig. 14G,H, can be related to c-axes orientation obtained by RALSER et al. (1991, Fig. 9) from coaxially strained quartz mylonite. The diagram 13 G resembles to crossed-girdle pattern and the diagram 14 H to pure shear models (LISTER & HOBBS, 1980).

#### 2.5. The Shape of the Orthogneiss Body from Gravity Interpretation

The interpretation was based on the density data (Table 3) of BEDNÁŘ & FRYÁKOVÁ (1971), ZIKMUND (1980) and on the best quality density data from the Choustník-1 and Choustník-2 300 and 400 m deep



Text-Fig. 12.  
Plot of the displacement vs. shear zone thickness in the younger shear zone.

boreholes. The differential density of the orthogneiss slightly decreases with depth. Considering the density distribution and geological structure, the value  $-0.090 \text{ gcm}^{-3}$  was chosen for interpretation.

Filtration by hand-smoothing was performed on Bouguer maps where  $\sigma_{\text{red}} = 2.69 \text{ gcm}^{-3}$ . Great accuracy is essential as the total course of isanomals in the study area and the wide range of wavelengths do not allow explicit definition of the shape of the regional gravity field. In addition, the actual gravity effect of the orthogneiss body (first unit of  $\mu\text{ms}^{-2}$ ) is hard to distinguish from the noise. Of the possible solutions, three types of regional field with slightly different curvature were chosen for quantitative interpretation.

The axis of the gravity low in the area changes from SW-NE to S-N. Judging from the character of the residual fields, the dimension of the tectonic klippe of the orthogneiss body grows with depth and the body

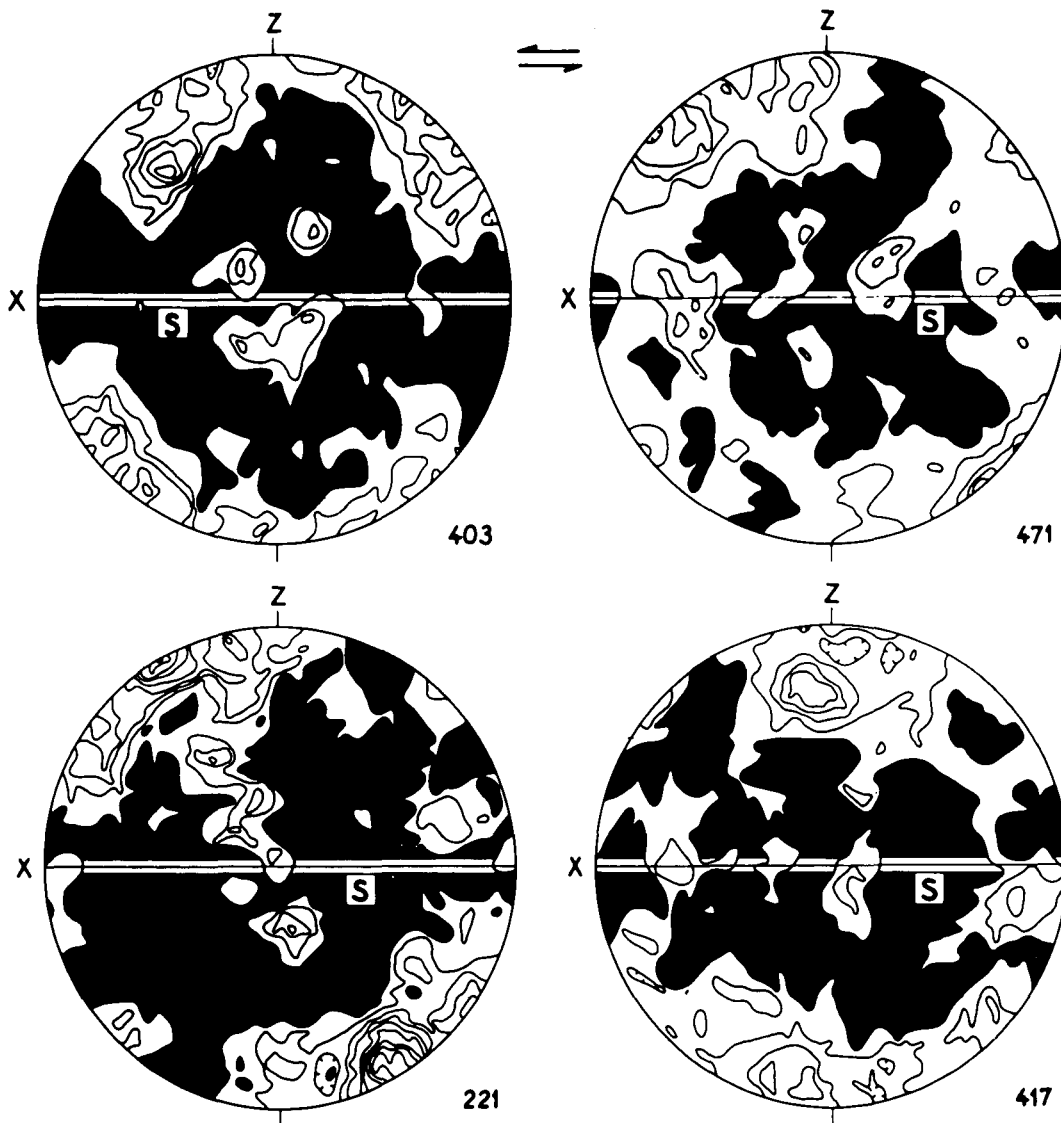
extends beneath the surface in the S-N direction, across the boundaries defined by the geological mapping.

Three lines were drawn so as to pass through the above-mentioned boreholes. Quantitative interpretation was subsequently performed on a HP-9845 desk-computer using the Talwani method for a two and a half dimensional body, i.e. a body given in the plane by the X-coordinates, h for intersections of edges and limited in the direction of its prolongation by vertical planes at respective distances. The inverse problem was solved for the real course of terrain. The results illustrated in Figs. 15A-F depict the models with the best agreement between the measured and the calculated curves.

The Choustnik orthogneiss body has an approximately plate flat "undulated" shape and dips gently to NW-N with an approximate angle of  $15^\circ$  in concert with its interpretation as a klippe of the tectonically

Table 3.  
Density data from the Choustnik orthogneiss.

Depth interval [m]	Rock type	Number of cores	Average density [ $\text{g/cm}^3$ ]		Porosity [%]
Borehole Choustnik-1					
0-34.5 (137.8)	Garnet amphibolite	4	3.18	3.19	0.425
137.8-247.2	Migmatized paragneiss	14	2.72	2.73	0.48
257.7-292.5	Orthogneiss	5	2.64	2.66	0.78
Borehole Choustnik-2					
0 - 94.5	Orthogneiss	9	2.61	2.64	1.38
109.9-403.7	Migmatized paragneiss	16	2.73	2.75	0.55



Text-Fig. 13.  
C-axes preferred orientation patterns in the tectonites of younger shear zones.  
Number of measurements in the lower right-hand corner, 1 % contours interval.

dismembered original batholith emplaced during thrust tectonics. The original thickness should be at least several kilometers (VIGNERESSE, 1988).

## 2.6. Rb-Sr Dating

To date, only the Bechyně orthogneiss (FEDIUK, 1976) has been dated in this area of the Central European Hercynian belt (VAN BREEMEN et al., 1982). The orthogneiss belongs to a distinct thrust zone some 25 km distant from the zone containing the Choustník orthogneiss. Moreover, the significance of the Rb-Sr age of  $489 \pm 19$  Ma. for this unit is not clear because of the possible opening of isotopic system during shearing. The relatively undeformed granites from the central part of the Choustník orthogneiss, however, can constitute material suitable for the dating of the intrusion age. Other determinations can be carried out simultaneously such as: the lower age limit of the shearing of the orthogneiss and the surrounding rocks, checking the previously reported Ordovician data from the Bechyně orthogneiss and dating of later Hercynian metamorphism.

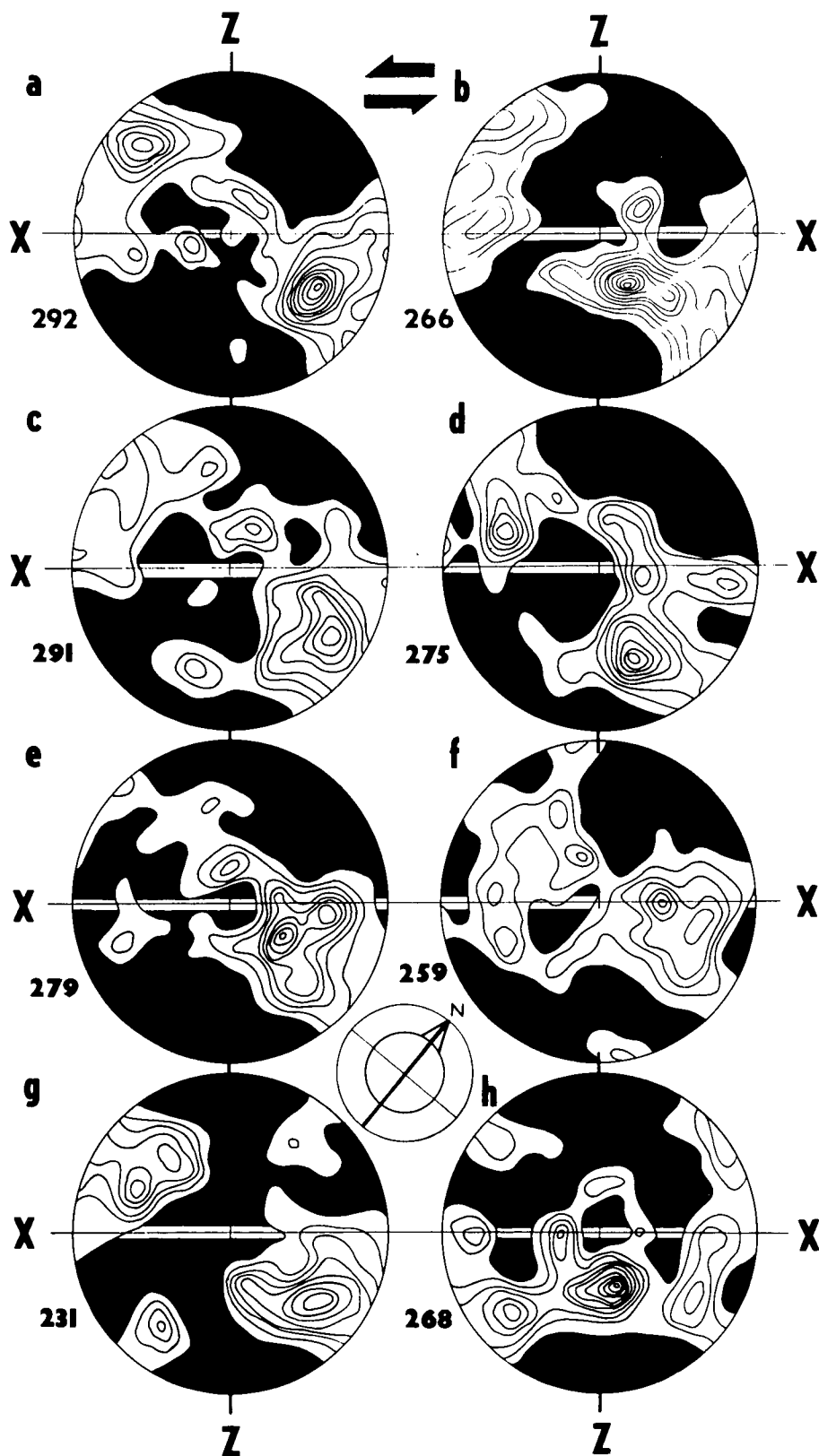
Seven samples of isotropic granites and two sheared granites were analyzed. Powders were obtained from crushing large fresh samples (30 to 50 kg) from the

coarse grained portions of the granite. Rb and Sr contents were determined by the isotope dilution method and decay constants of  $^{87}\text{Rb} = 1.42 \times 10^{-11} \text{an}^{-1}$  was used. Analytical details can be found in PEUCAT et al. (1988).

Nine samples gave an isochrone age of  $459 \pm 10$  Ma., with an initial ratio of  $0.712 \pm 2$  and MSWD of 5 (Fig. 16,

Table 4.  
Rb-Sr analyses of the whole rock samples of the Choustník orthogneiss.  
8414 to 8431 = undeformed samples; 8435 and 8438 = sheared granites.

Samples	Rb [ppm]	Sr [ppm]	$^{87}\text{Rb}/^{86}\text{Sr}$	$^{87}\text{Sr}/^{86}\text{Sr}$ [ $\pm 2 \sigma_m$ ]
8414	425	21.1	60.9	$1.11254 \pm 8$
8420	471	21.5	65.9	$1.13700 \pm 7$
8424	531	11.6	145	$1.6475 \pm 12$
8425	466	21.7	64.7	$1.13448 \pm 7$
8426	460	11.8	122	$1.5085 \pm 4$
8427	246	51.2	14.0	$0.80809 \pm 4$
8431	508	14.2	111	$1.4509 \pm 3$
8435	260	70.45	10.8	$0.78075 \pm 5$
8438	185	70.6	7.63	$0.76242 \pm 6$

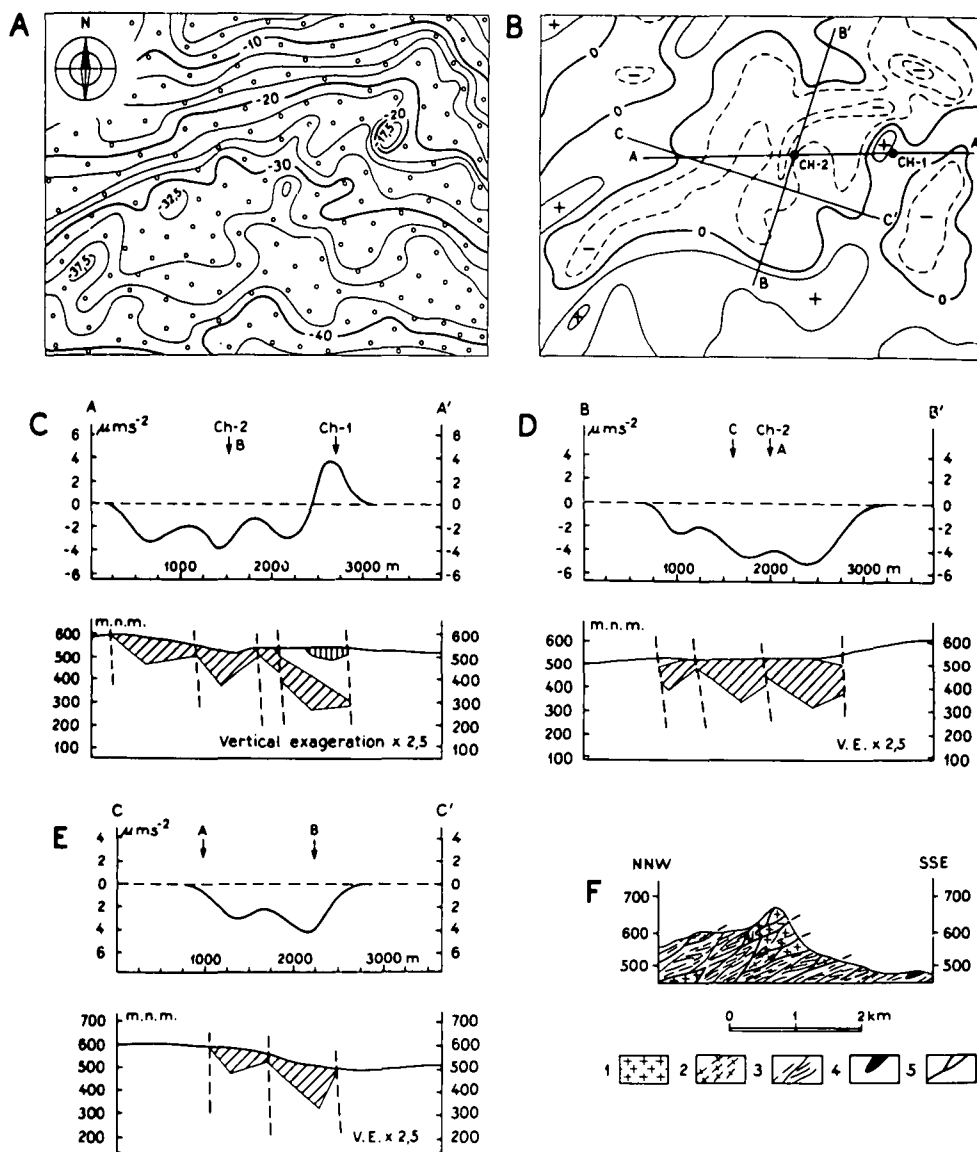


Text-Fig. 14.  
C-axes preferred orientation in the NE-SW stretching lineation bearing quartzites. E + 2 $\sigma$  contours interval; number of measurements in the lower left-hand corner.

Table 4). The high  $^{87}\text{Sr}/^{86}\text{Sr}$  initial ratio indicates a large degree of ancient crustal reworking at the source of the granite. Sheared samples do not show any evidence of opening of the Rb-Sr system. Although strongly supported by the dated Lower Ordovician extensional magmatism in surrounding areas the age obtained is interpreted here as the minimal intrusive age because of the high Rb/Sr ratio in the orthogneiss which can lead to the age underestimation (PIN, in print).

### 2.7. K-Ar Cooling Ages of Muscovite and Biotite

Three rock types, i.e., relict coarse-grained granite-porphphy (CH-03), fine grained central part of the sub-vertical shear zone in the relict granites (CH-05), and a fine- to medium-grained xenolith in metagranite (CH-07), Table 6, were chosen for the analyses. The fresh rock samples (30–50 kg) were crushed to 0.4–0.215 and 0.25–0.125 mm grain size fractions;



micas were separated on a Rapid and Cook electromagnetic separator and further purified. The analyses were carried out using the volumetric and the isotope dilution methods. The model ages (Table 5)

were calculated using the decay constants suggested by STEIGER & JÄGER (1973). Chemical analyses of the rock samples are given in Table 6.

Text-Fig. 16.  
Rb-Sr isochrone diagram of the Choustnik orthogneiss.  
The sample numbers are identical with the sampling points in Text-Fig. 3.

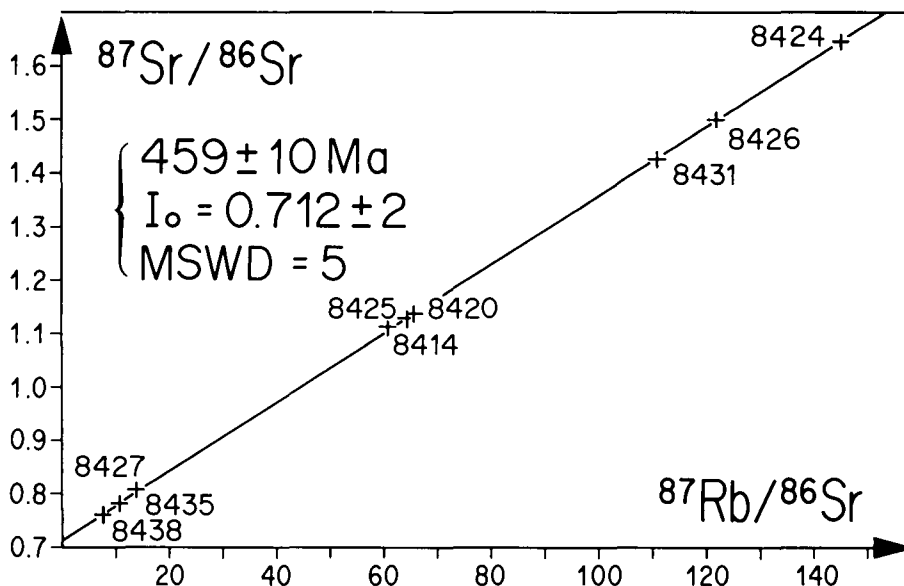




Table 5.

Geochronological analyses of muscovites and biotite from the Choustník orthogneiss. 8414 to 8431 = undeformed samples; 8435 and 8438 = sheared granites.

Sample	Analysed	$^{40}\text{Ar}_{i.d.}$ [ $10^{-12}\text{N}\cdot\text{m}^3\cdot\text{g}^{-1}$ ]	$^{40}\text{Ar}_{v.}$ [ $10^{-12}\text{N}\cdot\text{m}^3\cdot\text{g}^{-1}$ ]	K [%]	$t_{i.d.}$ [Ma]	$t_{v.}$ [Ma]
CH-03 (relict coarse grained granite porphyry)	Muscovite	97.83	95.61 ± 0.59	7.63 ± 0.08	303 ± 3	297 ± 6
CH-05 (fine grained central part of the subvertical shear zone)	Muscovite	89.22	90.76 ± 0.97	7.73 ± 0.09	275 ± 3	279 ± 6
CH-07 (medium grained metagranite; xenolith)	Biotite	98.55	101.88 ± 0.89	7.44 ± 0.08	312 ± 3	322 ± 6

$^{40}\text{Ar}_{i.d.}$ ,  $t_{i.d.}$  = argon and age determined by the isotope dilution method.

$^{40}\text{Ar}_{v.}$ ,  $t_{v.}$  = argon and age determined by the volumetric method.

Ma =  $10^6$  m. y.

The new K–Ar ages date the cooling to the blocking temperatures of the system (DODSON, 1973) which are assumed for biotite to be 300–345°C (DALLMAYER, 1978), 300±50°C (WAGNER et al., 1977) or 270°C (HARRISON et al., 1979); The muscovite blocking temperature is estimated to be 380°C by JÄGER (1973). The decrease to these temperatures in the Choustník orthogneiss occurred at 280 Ma.; the other ages obtained (303 and 312 Ma) are thought to be influenced by Ar contamination.

The Rb–Sr dating of the muscovite in the similar Bechyně orthogneiss by VAN BREEMEN et al. (1982) yielded an age range of 326 to 338 Ma. The decrease of 100–200°C (the blocking temperature of the Rb–Sr system in muscovite was estimated at 500°C by FAURE, 1987) in this area probably corresponds to a 30 to 50 Ma. time span.

### 3. Discussion

The Rb–Sr age of the Choustník orthogneiss is comparable with the 489±13 Ma. age for the Bechyně orthogneiss (VAN BREEMEN et al., 1982) and especially with the Ordovician volcanites of the Křivoklát – Rokycany area (490 Ma., VIDAL et al., 1975, Table 7). We consider this as supporting evidence for a Sardinian, Bohemian, or Lakslandian (MISAŘ et al., 1983) magmatic event in the crystalline rocks of the Bohemian Massif. Similar orthogneisses are, in fact, found in several places (Sněžník orthogneiss 487 Ma. ± 11, VAN BREEMEN et al., 1982) and they are generally very coarse-grained. They can be tentatively explained as the deep crustal parts of the Upper Cambrian – Lower Ordovician volcanic rocks.

The age of Variscan shearing of the orthogneiss which occurs in the vicinity of eclogite bodies is constrained by the preliminary data on the eclogite

metamorphism in the Bohemian Massif (338 Ma., Dobešovice; 374 Ma., Níhov; BRÜCKNER et al., 1989), Nd–Sm data (by 330 Ma), U/Pb in zircons (PEUCAT, preliminary data), by the 330 Ma. Rb–Sr age of muscovites

Table 6.

Chemical analyses of the investigated rocks.

Analyst: M. HUKA et al., Geological Survey Prague.

	CH – 03	CH – 05	CH – 07
SiO <sub>2</sub> [%]	75.83	76.39	73.98
TiO <sub>2</sub>	0.14	0.17	0.41
Al <sub>2</sub> O <sub>3</sub>	12.52	12.67	13.27
Fe <sub>2</sub> O <sub>3</sub>	0.07	0.41	0.14
FeO	1.29	1.28	1.74
MnO	0.027	0.028	0.034
MgO	0.25	0.37	0.30
CaO	0.44	0.41	0.68
Li <sub>2</sub> O	0.022	0.024	0.026
Na <sub>2</sub> O	2.78	2.32	3.09
K <sub>2</sub> O	4.75	4.90	4.49
P <sub>2</sub> O <sub>5</sub>	0.19	0.19	0.16
CO <sub>2</sub>	0.01	0.01	0.02
C	0.05	0.06	0.04
H <sub>2</sub> O <sup>+</sup>	0.77	1.00	0.77
F	0.18	0.22	0.21
S	0.03	0.02	0.02
H <sub>2</sub> O <sup>-</sup>	0.12	0.13	0.20
	99.47	100.59	99.58
F – ekv.*)	– 0.08	– 0.09	– 0.09
Total	99.39	100.49	99.49

\*) Correction for fluor/oxygen ratio.

Table 7.

Rb–Sr ages and other data of Ordovician rocks of the Bohemian Massif.

	Age	M.S.W.D.*)	Initial
Krivoklát-Rokycany Upper Cambrian rhyolites and porphyries (VIDAL et al., 1975)	490 ± 14	11	0.7041
Bechyně orthogneiss**) (VAN BREEMEN et al., 1982) Muscovites	489 ± 13 338 ± 8 – 326 ± 9	8.8	0.7068
Choustník orthogneiss (this paper)	459 ± 10	5	0.712
Sněžník orthogneiss (VAN BREEMEN et al., 1982)	487 ± 11		0.7069

\*) Mean standard weighted deviation.

\*\*) The age of this orthogneiss was recalculated after the data in Table 3 of VAN BREEMEN et al. (1982). All ages are calculated using the same 2σ error program.

**Table 8.**  
Age relationships of rocks in the Choustník area.

Age	Metamorphism	Intrusions	Shearing events and structures
460–490		Choustník and Bechyně granites	
370–390	Eclogites Micaschists (11 in Fig. 2) Garnet amphibolites		N–S to NW–SE thrusting
336		Durbachites (5a,b in Fig. 2)	NW normal faulting
330	Cooling	Non deformed granites (4 in Fig. 2)	
280		Closing of K/Ar system	

in the Bechyně orthogneiss (VAN BREEMEN *et al.*, 1982), and by the 336 Ma.  $^{39}\text{Ar}/^{40}\text{Ar}$  age of normal faulted durbachites (MATTE *et al.*, 1990).

The most reliable shear criteria for the earlier (thrusting) kinematics – left hand shear sense for the NE–SW oriented subhorizontal lineation in the northwesterly inclined foliation (Fig. 15) – provided the quartzites found northerly of the orthogneiss. The bulk kinematics in the earlier stage of shearing is thus top to S–SE thrusting of micaschists over paragneisses with granites and eclogites at the boundary.

The two N–S to NW–SE and NE–SW trends of the stretching lineation can be interpreted in terms of the structural fan (EMMONS, 1967) and/or transpression (RAMSAY & HUBER, 1987) leading to thrusting in the earlier stage in the sinistral strike-slip zone. This zone later underwent a crustal extension followed immediately by the intrusion of large bodies of Hercynian undeformed granites.

#### 4. Conclusions

The 90 m thick thrust klippe of the pre-Variscan Choustník (460 Ma.) porphyry granite of crustal origin in the Moldanubian of the Bohemian Massif was sheared in two principal Variscan events; firstly in NW–SE to N–S oriented thrusting and by later normal faulting. The latter event in the amphibolite facies metamorphism was followed by 330 Ma. intrusion of undeformed granites. This orthogneiss provides an example of the Variscan polyphase kinematics of the Moldanubian terrane of the Bohemian Massif.

#### Acknowledgements

The authors wish to thank the C.A.E.S.S.–C.N.R.S. and ASP Blocs and collisions (INSU) in France for financial support for this study. Special thanks go to Mrs. N. MORIN for technical assistance, Mrs. H. FICHET for the typing of the manuscript, Mrs. LAUTRAM for the careful drawing of the figures, Dr. RODE GAYER for the correction of the English and Dr. M. KLECKA for the help with the sampling.

#### References

- ARTHAUD, F.: Détermination graphique des directions de raccourcissement, d'allongement et intermédiaire d'une population de failles. – *Bull. Soc. Géol. Fr.*, 7 Sér. 11, 729–737, Paris 1969.
- ANDRIAN, F.v.: Beiträge zur Geologie des Kauřimer und Taborer Kreises in Böhmen. – *Jahrbuch der Geol. Reichsanst.*, 13, II, 155–182, Wien 1863.
- BADHAM, J.: Strike-slip orogens. An explanation for the Hercynides. – *J. Geol. Soc. London*, 139, 223, 493–504, London 1982.
- BARD, J.P., BURG, J.P., MATTE, PH. & RIBEIRO, A.: La chaîne hercynienne d'Europe Occidentale en termes de tectonique des plaques. – *Mém. B.R.G.M.*, 108, 26 IGC, C.6, 233–246, Paris 1980.
- BEDNÁR, J. & FRIÁKOVÁ, O.: Gravity measurements on locality Choustník. – MS Geofyzika (unpublished report), Brno 1971.
- BEHR, H.J.: Subfluenzprozesse im Grundgebirgsstockwerk Mitteleuropas. – *Z. Dtsch. geol. Gesell.*, 129, 283–318, Hannover 1978.
- BEHR, H.J.: Subduktion oder Subfluenz im Mitteleuropäischen Varistikum. – *Berl. Geowiss. Abh.*, R. A., 19, A. Wegener Symposium, 22–23, Berlin 1980.
- BERNARD, A.J.: Geological formations and rocks in surroundings of Tábor. – *Výr. Zpr. c. k. Gym. r. 1908–1909*, Tábor 1909 (in Czech).
- BRÜCKNER, H.K., MEDARIS, L.G.Jr. & BAKUN-CZUBAROW, N.: Nd and Sm age and isotope patterns from Hercynian eclogites and garnet pyroxenites of the Bohemian Massif and the east Sudetes. – *Terra Cognita Abstracts* 1, Abstr. 10, p.4., Strassbourg 1989.
- ČECH, V. *et al.*: Explanatory notice to the geological map of 1:200,000, Č. Budějovice and Vyšší Brod Sheets. – Geological Survey of Czechoslovakia (in Czech), Prague 1962.
- CALOUPSKÝ, J.: Tectonostratigraphic units of the Bohemian Massif. – *Čas. Min. Geol.*, 31, 4, 387–393, Prague 1986 (in Czech).
- DALLMAYER, R.D.:  $^{40}\text{K}/^{39}\text{Ar}$  incremental-release ages of hornblende and biotite across the Georgia inner Piedmont: their bearing on late Paleozoic-early Mesozoic tectonothermal history. – *Am. J. Sci.*, 278, 124–149, New Haven 1978.
- DELL'ANGELO, L.N. & TULLIS, J.: Fabric development in experimentally sheared quartzites. – *Tectonophysics*, 169, 1–21, Amsterdam 1989.
- DIETER, G.E.: *Mechanical metallurgy*. – pp. 774, New York etc. (McGraw Hill) 1976.
- DODSON, M.H.: Closure temperature in cooling geochronological and petrological systems. – *Contrib. Mineral. Petrol.*, 40, 259–274, Berlin 1973.
- EMMONS, R.C.: Strike-slip rupture patterns in sand models. – *Tectonophysics*, 7/1, 71–87, Amsterdam 1967.
- FAURE, G.: *Principles of isotope geology*. – pp. 589, New York (J. Wiley) 1986.
- FEDIUK, F.: The Bechyně "orthogneiss". Anatectic type of Moldanubian orthogneissoids. – *Acta Univ. Carol., Geol.*, 3, 187–207, Prague 1976.
- FRANKE, W.: Tectonostratigraphic units in the Variscan belt of central Europe. – *Geological Society of America Special Paper*, 230, 67–90, New York 1989.

- GAPAIS, D.: Shear structures within deformed granites: Mechanical and thermal indicators. – *Geology*, **17**, 1144–1147, Boulder 1989a.
- GAPAIS, D.: Les Orthogneiss: Structures, mécanismes de déformation et analyse cinématique. – *Mémoires et Documents du C.A.E.S.S.*, No. **28**, 1–366, Rennes 1989b.
- GAPAIS, D., BALE, P., CHOUKROUNE, P., COBBOLD, P.R., MAHJOUR, Y. & MARQUER, D.: Bulk kinematics from shear zone patterns: some field examples. – *Jour. Struct. geol.*, **9**, 5/6, 635–646, Oxford 1987.
- HARRISON, T.M., AMSTRONG, R.L., NEASER, C.W. & HARAHA, J.E.: Geochronology and thermal history of the Coast Plutonic Complex, near Prince Rupert, British Columbia. – *Can. J. Earth Sci.*, **16**, 3, 400–410, Ottawa 1979.
- JÄGER, E.: Die alpine Orogenese im Lichte der radiometrischen Altersbestimmungen. – *Eclogae geol. Helv.*, **66**, 1, 11–21, Basel 1973.
- KLEČKA, M., RAJLICH, P. & MELKA, R.: Ductile shear zones and origin of orthogneisses in the thrust sheet of Choustník. – *Acta Montana UGG ČSAV*, **72**, 35–62, Prague 1986.
- KLOMÍNSKÝ, J. & DUDEK, A.: The plutonic geology of the Bohemian Massif and its problems. – *Sbor. Geol. Věd, Geol.*, **31**, 47–69, Prague 1978.
- KNIPE, R.J. & LAW, R.D.: The influence of crystallographic orientation and grain boundary migration on microstructural and textural evolution in an S-C mylonite. – *Tectonophysics*, **135**, 155–169, Amsterdam 1987.
- KREBS, W.: The tectonic evolution of Variscan meso Europa. – In: D.V. AGER & M. BROOKS (eds.): "Europe from crust to core", New York (John Wiley) 1977.
- KREJČÍ, J.: Geology or the Science of the Earth Forms with Special Regard to the Czech Countries. – Prague 1877 (in Czech).
- LEE, J., MILLER, E.S. & SUTTER, J.F.: Ductile strain and metamorphism in an extensional tectonic setting: a case study from the northern Snake Range, Nevada. – In: COWARD, M.P., DEWEY, J.F. & HANCOCK, P.L. (eds.): "Continental Extensional Tectonics". – *Geol. Soc. Spec. Publ.*, **28**, 267–298, London 1987.
- LISTER, G.S. & HOBBS, B.E.: The simulation of fabric development during plastic deformation and its application to quartzite: the influence of deformation history. – *Jour. Struct. Geol.*, **2**, 3, 355–370, Oxford 1980.
- MARQUER, D.: Structures et déformation alpine dans les granites hercyniens du massif du Gotthard (Alpes centrales suisses). – *Eclogae geol. Helv.* **83**/1, 77–97, Basel 1990.
- MATTE, PH.: Tectonics and plate tectonics model for the Variscan belt of Europe. – *Tectonophysics*, **126**, 329–374, Amsterdam 1986.
- MATTE, PH. & BURG, J.P.: Sutures, thrusts and nappes in the Variscan arc of Western Europe: plate tectonic implications. – In: *Thrust and Nappe Tectonics*, 353–357, London 1981.
- MATTE, PH., MALUSKI, H., RAJLICH, P. & FRANKE, W.: Terrane boundaries in the Bohemian Massif: result of large-scale Variscan shearing. – *Tectonophysics*, **177**, 151–170, Amsterdam 1990.
- MISAŘ, Z., DUDEK, A., HAVLENA, V. & WEISS, J.: Geology of Czechoslovakia, Part I, SPN. – Prague 1983 (in Czech).
- OBERC-DZIEDZIC, T.: The development of gneisses and granites in Eastern part of the Ižera crystalline unit in the light of the textural investigations. – *Acta Universitatis Wratislaviensis*, No. 997. *Prace Geologiczno-mineralogiczne XIII*, 1–181, Wrocław 1988.
- PAQUETTE, J.L.: Comportement des systèmes isotopiques U-Pb et Sm-Nd dans le métamorphisme écolitique, chaîne hercynienne et chaîne alpine. – *Mém. et doc. du C.A.E.S.S. Rennes*, **14**, 189p, Rennes 1987.
- PEUCAT, J.J.: Géochronologie des roches métamorphiques (Rb-Sr et U-Pb). Exemples choisis au Groënland, en Laponie, dans le Massif armoricain et en Grande Kabylie. – *Mém. Soc. Géol. Minéral. Bretagne*, **28**, 158 p., Rennes 1983.
- PEUCAT, J.J., VIDAL, PH., GODARD, G. & POSTAIRE, B.: Precambrian U-Pb zircon ages in eclogites and garnet pyroxenites from South Brittany (France): an old oceanic crust in the West European hercynian belt? – *Earth Plan. Sc. Lett.* **60**, 70–78, Amsterdam 1982.
- PIN, C.: Il Central Western Europe: Major Stages of Development During Precambrian and Paleozoic Times. – In: R.D. DALLMAYER & J.P. LÉCORCHÉ (eds): "Geology of the West African Orogens and Circum Atlantic Correlation". – IGC Project 233 "Terranes in the Circum Atlantic Paleozoic Orogens", 278–289, (Springer Verlag) (in print).
- RAJLICH, P.: Variszische duktile Tektonik im Böhmischem Massiv. – *Geologische Rdsch.*, **76**, 3, 755–786, Stuttgart 1987.
- RAJLICH, P.: Strain analysis of Devonian fossils from the NE part (Rhenohercynian zone) of the Bohemian Massif. – *Annales Tectonicae*, **III**, 1, 44–51, Firenze 1989.
- RAJLICH, P. & SYNEK, J.: A cross-section through the Moldanubian of the Bohemian Massif and the structural development of its ductile domains. – *N. Jb. Paleont. Mh.*, **11**, 689–698, Stuttgart 1987.
- RALSER, S., HOBBS, B.E. & ORD, A.: Experimental deformation of a quartz mylonite. – *J. Struct. Geol.*, **13**, 7, 837–850, Oxford 1991.
- RAMSAY, J.G. & HUBER, I.: The Techniques of Modern Structural Geology, Vol. 2: Folds and Fractures. – 1–700, London (Academic Press) 1987.
- ŠAFRÁNEK, F.: Geognostic and Geological Overview of the Tábor district. – Annual Report of the Gymnasium of Tábor, Tábor 1878 (in Czech).
- STILLE, M.: Das Mitteleuropäische variszische Grundgebirge im Bilde des gesamteuropäischen. – *Geol. Jb., Beih.* **2**, 138, Hannover 1951.
- STUR, D.: Die Umgebung von Tabor (Wotitz, Tabor, Jung-Woschitz, Patzau, Pilgram und Čechtitz). – *Jahrbuch der Geol. Reichsanst.*, **IX**, 661–688, Wien 1858.
- SVOBODA, J. et al.: Regional Geology of Czechoslovakia, Part I, The Bohemian Massif. – 1–668, Geol. Survey, Prague 1966.
- ŠMEJKAL, V. & MELKOVÁ, J.: Notes on some potassium argon dates of magmatic and metamorphic rocks from the Bohemian Massif. – *Čas. Min. Geol.*, **14**, 3–4, 331–338, Prague 1969.
- VAN BREEMEN, O., AFTALION, M., BOWES, D.R., DUDEK, A., MISAŘ, Z., POVONDRA, P. & VRANA, S.: Geochronological studies of the Bohemian Massif, Czechoslovakia, and their significance in the evolution of Central Europe. – *Trans. Roy. Soc. of Edinburgh*, **73**, 80–108, Edinburgh 1982.
- VAUCHEZ, A.: The development of discrete shear zones in a granite: stress, strain and changes in deformation mechanisms. – *Tectonophysics*, **133**, 137–156, Amsterdam 1987.
- VIDAL, PH., AUVRAY, B., CARLOT, R., FEDIUK, F. & HAMEURT, J.: Radiometric age of volcanics of the Cambrian "Křivoklát-Rokycany" complex (Bohemian Massif). – *Geologische Rdsch.*, **64**, 2, 563–570, Stuttgart 1975.
- VIGNERESSE, J.L.: Forme et volume des plutons granitiques. – *Bull. Soc. Géol. France*, 1988 (8), **IV**, 6, 897–906, Paris 1988.
- WAGNER, G.A., REIMER, G.M. & JÄGER, E.: Cooling ages derived by apatite fission track, mica Rb-Sr and K-Ar dating: the uplift and cooling history of the central Alps. – *Societa Cooperativa Tipografica, Padova* 1977.
- WHITE, S.H.: Chrupkije deformaciji v plastičeskich zonach razlomov. – 27 IGC, Section C.07, Dokl. 7, Nauka, Moscow 1984.

YU, H. & ZHENG, Y: A statistical analysis applied to the  $Rf/\phi$  method. - *Tectonophysics*, **110**, 151-155, Amsterdam 1984.

ZIKMUND, J.: Final report on structural boreholes Choustník-1 and 2. - Manuscript, Archives ÚÚG (unpublished report), Prague 1980.

ZIKMUND, J.: Relict granites and genesis of the Blaník type orthogneisses. - *Čas. Min. Geol.*, **28**, 1, 81-87, Prague 1983.

ZOUBEK, V., COGNÉ, J., KOZHOUKHAROV, D. & KRÄUTNER, H.: Precambrian in Younger Fold Belts, European Variscides, the Carpathians and Balkans. - 1-885, New York (J. Wiley & Sons) 1988.

ŻELAZNIEWICZ, A.: Orthogneisses due to irrotational extension, a case from the Sudetes, Bohemian Massif. - *Geologische Rdsch.*, **77**, 3, 671-682, Stuttgart 1988.

Manuskript bei der Schriftleitung eingelangt am 16. Oktober 1991.